PREDICTING OFF-SITE DEPOSITION OF SPRAY DRIFT FROM HORTICULTURAL SPRAYING THROUGH POROUS BARRIERS ON SOIL AND PLANT SURFACES

Geoff Mercer* and Tony Roberts†

Abstract

Shelterbelts can be used to capture spray drift from crop spraying and reduce its spread to non crop areas. Critical factors in the efficiency of this capture are the ambient wind velocity, the structure of the shelterbelt and the spray drift droplet distribution. Here we present a model of the flow through and over a shelterbelt. It is found that the flow pattern is largely independent of the ambient wind strength (velocity). Settling and evaporation of the spray drift droplets are investigated and critical droplet diameters determined. It is found that droplets larger than 200 μm settle before reaching the shelterbelt and need not be included in the shelterbelt capture calculations. A model of the spray drift collection within the shelterbelt is analysed. Wind speeds between 1 and 5 m/s are considered which is the range that spray operations are usually performed over. Shelterbelts with optical porosities between 10% and 30% and constructed of fine particles such as pine needles are found to perform the best.

1. Introduction

New Zealand is a recognized leader in horticultural practices which include the use of boundary shelterbelts around orchards such as those shown in Figure 1. These shelterbelts were primarily established to provide protection to the crop but more recently have been recognized as an effective means of ameliorating agrichemical spray drift that may arise from the crop production area. Shelterbelt structure ranges from large trees (ranging from broad leaf to needle in structure) to hedgerows and

*University of New South Wales, Canberra, ACT, Australia. E-mail: g.mercer@adfa.edu.au
†University of Southern Queensland, Toowoomba, Qld, Australia. E-mail: aroberts@usq.edu.au

artificial netting. The efficiency of the shelterbelt in capturing spray drift is known to depend on factors such as spray drift droplet size, wind velocity and the vegetation structure. However, more specific information and models are required to define the capture efficiency to develop a comprehensive spray drift management system.

The task set the MISG team was to investigate a mathematical model of the shelterbelt efficiency. Factors such as wind profiles through and above the shelterbelts, release height of the spray drift, capture efficiency of different droplet sizes and evaporation rates all need to be considered. The object of the exercise is to produce a better working model. Any model that is developed would need to be usable at the farm level. That is, any inputs to the model need to be easily measured or estimated quantities such as free stream wind velocity, optical porosity of the shelterbelt and typical vegetation element size of the shelterbelt.

We divide the problem into three main areas: firstly, the mean flow through and over the shelterbelt; secondly, the spray drift droplet size distribution and the effects of evaporation and settling; and thirdly, the capture efficiency within the shelterbelt as a function of the characteristics of the shelterbelt and the wind field. Each of these is considered in the following sections.

2. Wind flows in and over the shelterbelt

Figure 2 shows the streamlines for wind flowing over and through a crop and a shelterbelt: the wind flow decelerates through the shelterbelt, forcing a little wind over the shelterbelt, and provides shelter downstream of the shelterbelt in the weak recirculating region.

2.1. The wind is turbulent

The wind flowing over the earth has the well established logarithmic profile for its profile near the ground: $u \propto \log y$ where y is the height above the ground [2]. This logarithmic profile is a consequence of the strong turbulent nature of the wind mixing momentum vertically in the atmosphere. The driving force for the wind near the ground is thus the wind higher in the atmosphere: the pressure gradient is a negligible driving force in atmospheric dynamics (that the wind blows dominantly *along* isobars, not across them). It is for this reason that shelterbelts are so effective in providing shelter: there is no pressure forcing of the wind, only drag from above.

We explore the wind flow over and through crops and shelterbelts with a simple eddy viscosity model of mean turbulent flow: let $\boldsymbol{u}$ denote the mean wind velocity, and p denote the mean pressure field.

Figure 1. Some examples of shelterbelts and crop.

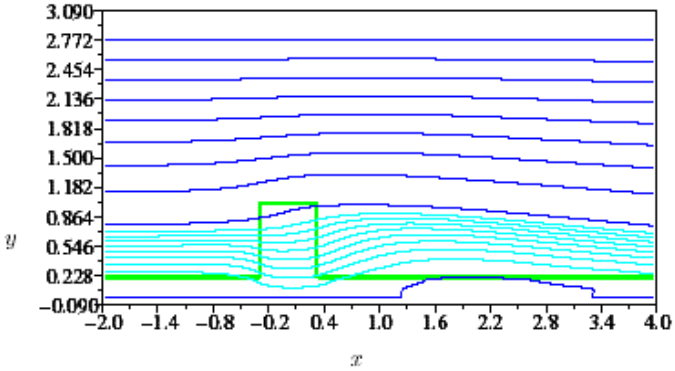

Figure 2. Streamlines of wind blowing over and through a crop and shelterbelt: multiple green lines outline the crop and shelterbelt boundary; the bottom (fainter) 9 streamlines are equispaced at 1/10 of the separation of the upper 9 streamlines to show more details of the flow near the ground (including a weak recirculation within the downwind crop). The flow is in the positive x-direction. The length x and y are nondimensionalised using shelterbelt height as a scale, here shown as unit height.

The incompressible fluid equations are then

$$\rho\left(\frac{\partial \boldsymbol{u}}{\partial t} + \boldsymbol{u}\cdot\boldsymbol{\nabla}\boldsymbol{u}\right) = -\boldsymbol{\nabla}p + \boldsymbol{\nabla}\cdot(\rho\nu_{\mathsf{T}}\boldsymbol{\nabla}\boldsymbol{u}) - \tfrac{1}{2}C_D\rho|\boldsymbol{u}|\boldsymbol{u}/\ell\,, \quad (1)$$

$$\boldsymbol{\nabla}\cdot\boldsymbol{u} = 0\,. \quad (2)$$

where ν_{T} represent some turbulent eddy viscosity that may vary in space and time, and C_D is a drag coefficient for flow through shelterbelts and crop which will vary in space (being zero in the air for example).[1]

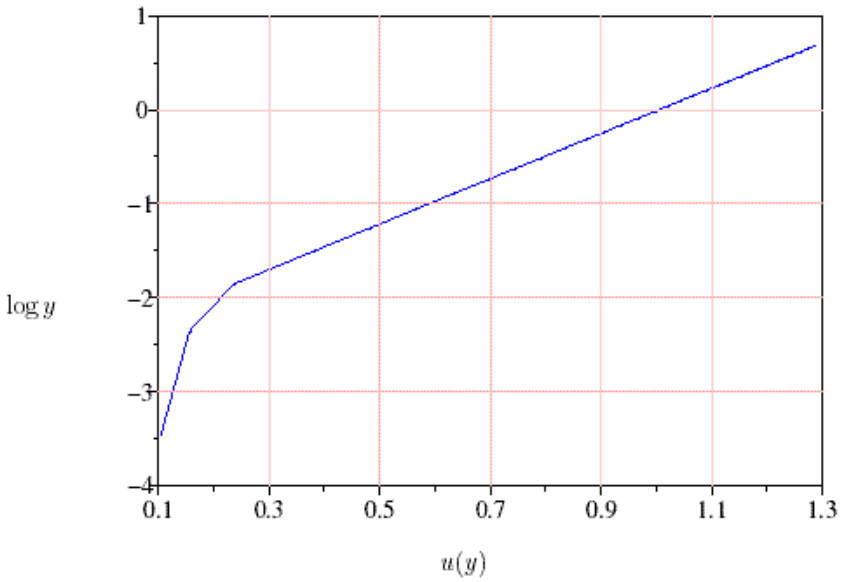

Figure 3. An example profile of mean horizontal velocity showing the logarithmic profile in the nearly linear dependence for larger y.

In the wind's atmospheric boundary layer over flat terrain the mean horizontal velocity [2, 4]

$$u(y) = \frac{1}{\kappa}u_\tau \log\frac{y}{y_0}\,, \quad (3)$$

where von Karmen's constant $\kappa = 0.4$, y_0 is some reference height depending upon the effective surface roughness of the ground, and the "friction velocity" $u_\tau = \sqrt{\tau/\rho}$ where τ is the wind stress that is being carried down to the ground by the turbulent shear flow. For example,

Figure 3 shows an ideal profile of the wind above a crop of nondimensional "roughness height" $y = 0.2$: see that the extrapolation of the logarithmic dependence to $u = 0$ gives a roughness height of $\log y_0 \approx -2.3$, that is, the roughness height $y_0 \approx 0.1$; the slope of the logarithmic dependence of about 0.43 indicates the applied wind stress is such as to make the dimensionless friction velocity $u_\tau \approx 0.17$. In the profile shown in Figure 3 this wind stress is indirectly specified by requiring the wind speed $u = 1$ at height $y = 2$, nondimensionally. In such a vertically varying profile of the wind, we have to be careful about where wind speed is measured: conventionally, wind speed is reported from measurements at 10 m height. The domain of our interest lies well within this boundary layer which typically holds well up to 100–200 m high [2].

Now turn to the turbulent eddy diffusivity ν_T and the structure it must have to give such realistic atmospheric boundary layers. From the vertical diffusion in the horizontal momentum equation for the mean steady shear flow with negligible pressure gradient

$$\frac{\partial}{\partial y}\left(\nu_\mathsf{T}\frac{\partial u}{\partial y}\right) = 0 \quad \text{has solutions} \quad u \propto \log y$$

only when we prescribe the eddy diffusivity

$$\nu_\mathsf{T} \propto y\,. \tag{4}$$

That is, through turbulence the atmosphere is effectively nearly "inviscid" near the ground and becomes progressively more "viscous" further from the ground—Figure 3 is generated with this eddy diffusivity.[2] This dependence of eddy viscosity with height also arises from Prandtl's turbulent mixing length being proportional to the distance from the ground: $l_m = \kappa y$ [8]. In our approximation to turbulent atmospheric flow we prescribe the eddy viscosity to depend linearly with height as in (4) and then solve for the mean flow.

Recall that turbulent flow is intermittent [1]. Indeed L. F. Richardson [7] famously wrote:

> Does the wind possess a velocity? The question, at first sight foolish, improves upon acquaintance.

Thus although we only consider mean flow, there will be significant departures from the mean that will occur from time to time in unpredictable gusts of wind. Such intermittency may not be always ignorable.

2.2. Nondimensionalise for analysis

To begin we will not be specific: suppose the characteristic mean velocity is U and the characteristic mean length scale is L. The reference

time $T = L/U$ and reference pressure ρU^2. Scale all physical quantities with respect to these scales; the nondimensional Navier–Stokes equations become

$$\frac{\partial \boldsymbol{u}}{\partial t} + \boldsymbol{u}\cdot\boldsymbol{\nabla}\boldsymbol{u} = -\boldsymbol{\nabla}p + \boldsymbol{\nabla}\cdot\left(\frac{\nu_{\mathsf{T}}}{UL}\boldsymbol{\nabla}\boldsymbol{u}\right) - \tfrac{1}{2}C_D\frac{L}{\ell}|\boldsymbol{u}|\boldsymbol{u}\,, \qquad (5)$$

$$\boldsymbol{\nabla}\cdot\boldsymbol{u} = 0\,. \qquad (6)$$

Choose the reference length to be the height of the shelterbelt, thus nondimensionally the shelterbelt height 1.

Here choose the velocity scale U to be the unobstructed mean wind speed at shelterbelt height L. Such a wind speed is the obvious scale, but in a logarithmic profile there is no definite wind speed (except the convention that the wind is usually measured at 10 m). Perhaps the velocity scale should be what the farmer might measure, but shelterbelts considerably change the airflow near the ground. The nondimensional turbulent eddy diffusion is implemented as $\nu_{\mathsf{T}} = 0.07\,y$. Look at an argument for this: Prandtl's mixing length argument [8] specifies the eddy diffusivity $\nu_{\mathsf{T}} = l_m^2|du/dy|$ where $l_m = \kappa y$; thus with the logarithmic profile and that the velocity scale is that at the mean velocity at height L; then

$$\frac{\nu_{\mathsf{T}}}{UL} = \kappa\frac{u_\tau y}{UL} = \frac{\kappa^2}{\log(L/y_0)}\frac{y}{L}\,.$$

Assuming $L/y_0 \approx 10$, this gives the nondimensional eddy diffusivity $\nu_{\mathsf{T}} = 0.07\,y$.

The boundary conditions on the wind are those of:

- at the inlet and outlet, fixed pressure p, $v = 0$ and $\frac{\partial u}{\partial x} = 0$ — the pressure would be zero we need some pressure drop to cater for the extra drag of the shelterbelt and so we determine the (small) pressure drop necessary to raise the horizontal fluid velocity to $u = 1$ at shelterbelt height $y = 1$;
- at the bottom are stress free conditions of $v = 0$ and $\frac{\partial u}{\partial y} = 0$ — the drag in the crop approximately provides a no-slip boundary condition for the air flow above;
- at the top $y = Y$ is a specified wind $u = U_Y$ and $v = 0$.

What should we supply for U_Y? In a logarithmic profile with velocity scale being that at the shelterbelt height $y = 1$

$$\frac{U_Y}{U} = \frac{\frac{1}{\kappa}u_\tau\log\frac{Y}{y_0}}{\frac{1}{\kappa}u_\tau\log\frac{1}{y_0}} = 1 + \frac{\log Y}{\log(1/y_0)}\,.$$

In our simulations with $Y = 2$ and $y_0 \approx 0.1$ the nondimensional prescribed wind at the top should be $U_Y/U = 1.3$. Remarkably, the geometry of the air flow through the crop and shelterbelt should be largely independent of the wind speed as we have nondimensional equations with no wind parameter appearing. One reason is that the turbulence scales with the velocity and so the eddy diffusivity scales with the inertial effects. Similarly, the quadratic drag scales with the inertia. Consequence, the same pattern of air flow appears for all wind speeds.

2.3. Quadratic drag in crops and shelterbelt

Whenever the air flows through the crop or shelterbelt, we apply a quadratic drag law as we assume the local Reynolds number based upon the leaf diameters is large enough for these to be reasonable. The quadratic drag law is implemented nondimensionally as $-\frac{1}{2}C_D(L/\ell)|\boldsymbol{u}|\boldsymbol{u}$ where the coefficient of drag C_D is zero in the free air, and a fixed constant in the crop and the shelterbelt depending upon the shape of the leaves. For most practical purposes we can take $C_D = 1$ [3] as this is about correct over a wide range of shapes and wide range of local Reynolds numbers.

The length parameter ℓ arises as the drag is proportional to the total cross sectional area of leaves per volume of shelterbelt and crop. Thus ℓ is the mean free path length of a fluid particle between "encounters" of a leaf in the shelterbelt and crop. Alternatively, consider that ℓ is the thickness of crop or shelterbelt that reduces the opacity to $1/e = 37\%$. Figure 4 shows the flow through a shelterbelt with $L/\ell = 20$.

2.4. Flows through different shelterbelts

We compute numerical solutions for the steady flow governed by the mean turbulent equations (5–6) on a 64×32 grid in the computational domain shown in Figures 2 and 4. This involves solving the nonlinear equations with a total of 6017 unknowns using a quasi-Newton method with a numerically approximated Jacobian (which is only recomputed whenever the norm of the residual does not decrease by a factor of 0.9). Recall from the discussion in Section 2.1 that the pressure gradient in the atmosphere is "negligible". In an infinite domain the pressure *drop* across a shelterbelt would cause a negligible change to the large scale pressure *gradient*. However, in our finite computational domain we do have to resolve the finite pressure drop across the hedge. Thus an outer iteration adjusts the mean pressure drop from the upwind to the downwind extremes of the domain; we use secant iteration to adjust the

pressure drop to ensure the upwind profile is close to the undisturbed turbulent logarithmic profile.

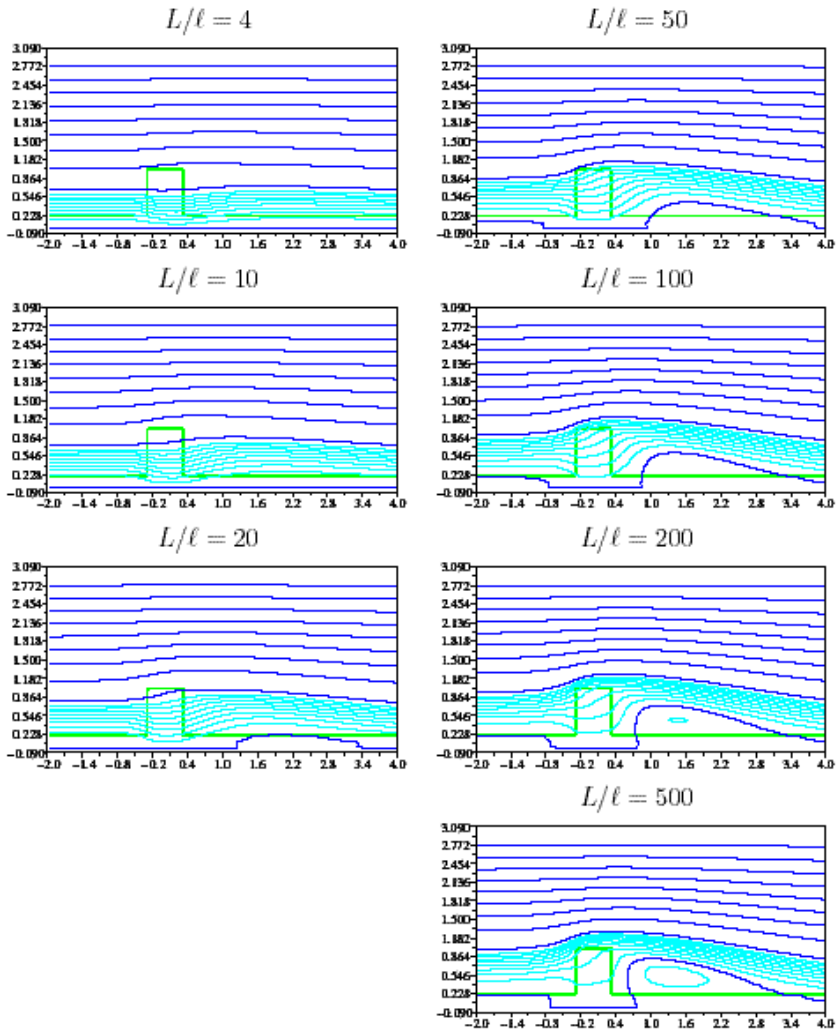

Figure 4. flow through shelterbelts and crop (outlined) with various thickness of vegetation, characterised by the porosity, and nondimensionally measured by the ratio of the hedge height to the mean free path, L/l. The flow through a shelterbelt with $L/\ell = 20$.

Look at the mean turbulent flows depicted in Figure 4. See that as the shelterbelt vegetation gets thicker, higher L/ℓ, the flow deviates more over the shelterbelt and a large downwind recirculation region develops. Ignore the small upwind recirculation region in the crop for high L/ℓ as we suspect it to be an artefact of the finite size of the computational domain. The crucial feature is the amount of upwind air which flows through the hedge and hence carries the spray that can be captured. See that up to $L/\ell \approx 100$ most of the upwind air will go through the full width of the shelterbelt—any spray kept below about 75% of the hedge height may be captured by the shelterbelt provided $L/\ell < 100$.

Figure 4 also shows that there can be significant flow down through the bottom of the shelterbelt, especially for the opacities most likely to be used to capture spray drift, approximately $10 < L/\ell < 100$. This is due to the significant pressure drop across the shelterbelt. If the shelterbelt does not reach the ground, as in the top-left shelterbelt in Figure 1, there will be significant transport of spray drift past the shelterbelt. Thus to best capture spray drift the shelterbelt must reach all the way down to the ground as in the other shelterbelts of Figure 4.

We also explored different shelterbelt widths. Figure 5 shows the flow through different shelterbelts. Doubling the width of the shelterbelt does not have as big an effect as doubling the vegetation density, doubling L/ℓ. Very wide shelterbelts push the air flow up as it flows through the shelterbelt, hence reducing the effectiveness of the shelterbelt in capturing spray drift. Figure 5 suggests that the shelterbelt should not be wider than its height.

3. Spray drift droplet distribution

The type of sprayer and its usage affects the distribution of droplets in the spray drift. Spray nozzles vary from very fine to coarse and the height and velocity of the spray application can also vary widely. What is important in determining the distribution of droplets in the spray drift impinging on the shelterbelt is the initial distribution of the droplets, their settling and their evaporation.

3.1. Settling

The droplets settle according to the Stokes settling velocity which is a balance between gravitational effects and their bouyancy and drag.

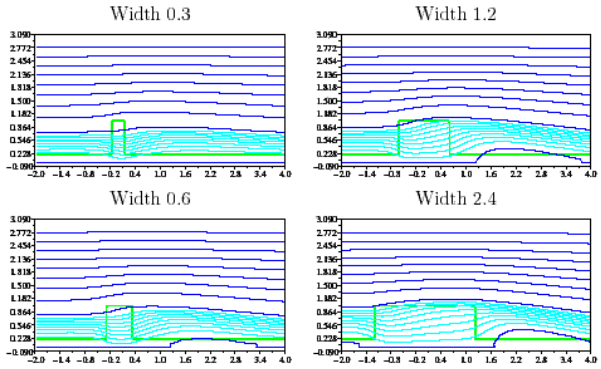

Figure 5. flow through shelterbelts and crop (outlined) with various widths of the shelterbelt, relative to the height; the vegetation density is $L/l = 20$.

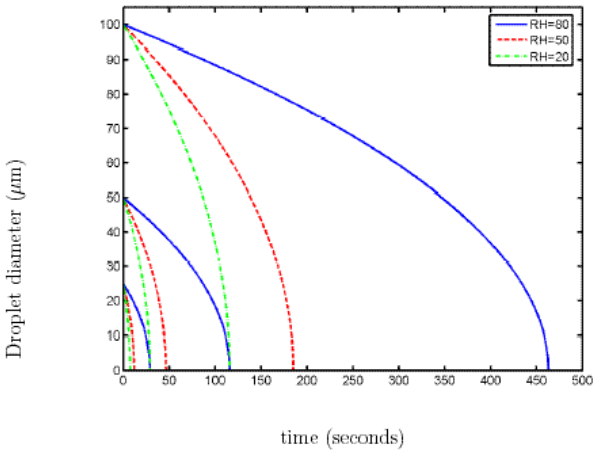

Figure 6. Evaporating droplet diameter as a function of time for three initial droplet sizes (25, 50, 100 μm) and three relative humidities.

The Stokes settling velocity

$$v_s = \frac{d_p^2 g(\rho_p - \rho_a)}{18\nu_a}\,, \tag{7}$$

where ρ_p is the density of the droplet, d_p the diameter of the droplet, ρ_a the density of the air, ν_a the kinematic viscosity of air and g the acceleration due to gravity. The important thing to note is that this

Table 1. Settling velocities and time to settle a height of 2.5 m for various droplet diameters.

Droplet size (μm)	Settling velocity (m/s)	Settling time (s)
10	0.003	827.5
20	0.012	206.9
30	0.027	91.95
50	0.076	33.10
100	0.302	8.275
200	1.208	2.069
300	2.719	0.920

varies with the square of the droplet diameter and ranges from 0.003 m/s for 10 μm droplets to 2.72 m/s for 300 μm droplets. See Table 1 for typical settling velocities for a variety of droplet diameters and their corresponding time to settle from a height of 2.5 m (a typical height of spray for crops such as kiwi fruit).

Consider a typical example of use in the field with the sprayer close to the shelterbelt. For a typical wind velocity at the crop level of 3 m/s, with a sprayer 6 m from the shelterbelt this gives a flight time of 2 s before the droplets reach the shelterbelt. If the spray is released at 2.5 m then droplets above 200 μm will have settled to the ground or target plant before they reach the shelterbelt. In reality most spraying is done at a greater distance from the shelterbelt and so larger droplets have even longer time to settle. Even if large particles do make it to the shelterbelt in the spray drift they are very efficiently captured there as shown in Section 4. In terms of spray drift the important part of the droplet distribution is the smaller droplet sizes as they do not settle out but are carried in the mean flow and are less efficiently captured by the shelterbelt.

3.2. Evaporation

As a droplet is carried along in the mean flow it evaporates depending on its current size and other factors such as the relative humidity. [10] derived a formula for the change in diameter of the droplet with time and a given relative humidity (RH) as

$$d_p = \sqrt{d_0^2 - \beta(100 - \mathrm{RH})t}\,, \tag{8}$$

where d_0 is the original droplet diameter and $\beta = 1.08 \times 10^{-12}\,\mathrm{m}^2/\mathrm{s}$ fitted from data. Figure 6 shows the change in droplet diameter as a function

of time for three different initial droplet diameters (25, 50 and 100 μm) and three different humidities (20%, 50% and 80%). For smaller droplets ($\leq 50\,\mu$m) the time scale of evaporation is in the order of 100 seconds which is relevant for capture in the shelterbelt as this is the time scale on which the spray drift is over the target crop. For larger droplets the time scales are more relevant to the spray drift that goes over the shelterbelt and is deposited far downstream.

4. Droplet collection in the shelterbelt

The capture efficiency of a porous shelterbelt depends on factors such as ambient wind velocity, wind velocity through the shelterbelt, droplet size in the incoming air flow, size, distribution and porosity of the shelterbelt material. Closely following [6] we develop a model for the deposition of particles onto the shelterbelt material for a given speed of flow through the shelterbelt. The assumptions in this model include that the wind flows horizontally through the shelterbelt and that there is no vertical variation in the wind flow or droplet concentration up the shelterbelt. The horizontal flow is reasonable except near the top of the shelterbelt as shown by the streamlines calculated in Section 2. This latter assumption presumes a relatively well mixed droplet concentration impinging on the shelterbelt and a reasonably uniform shelterbelt in height. These scenarios are frequently the case, see Figure 1.

4.1. Capture efficiency of individual shelterbelt elements

Consider a uniform shelterbelt of width W and height L with a velocity through the shelterbelt of U_b, this is often termed the bleed velocity as it is the component of the wind that 'bleeds' through the shelterbelt rather than going over the shelterbelt (see Section 2). There are three methods of deposition of droplets on to the shelterbelt elements; gravitational settling, Brownian motion and impaction due to the bleed flow. Gravitational settling is not significant within the shelterbelt as large particles that are subject to settling over the time span of interest have predominantly settled out by the time the spray drift reaches the shelterbelt and the majority of the remaining particles are small enough that they are carried with the ambient flow (see Section 3). Brownian motion is only significant for particles smaller than 0.1 μm in diameter and so is not relevant here. Hence the major source of droplet capture is by impaction on to vegetation elements.

As fluid flows around a shelterbelt element small particles are swept up with the flow while larger particles with more inertia will deviate

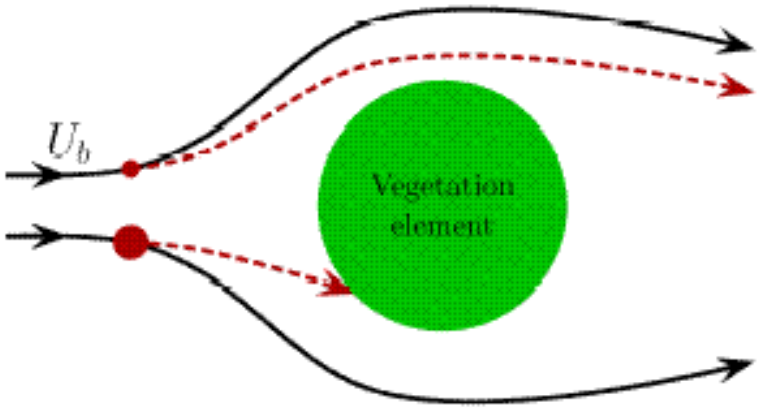

Figure 7. Large particles are possibly carried by their inertia into shelterbelt elements whereas lighter particles more closely follow the flow and may miss.

from the flow and possibly impact on the vegetation and be captured, see Figure 7. [5] derived an empirical formula for the efficiency E of this capture,

$$E = \left(\frac{\mathrm{St}}{\mathrm{St} + 0.8}\right)^2, \tag{9}$$

based on the the Stokes number St of the flow

$$\mathrm{St} = \frac{\rho_p d_p^2}{18\rho_a \nu_a} \frac{2U_b}{d_e} \tag{10}$$

where U_b the bleed velocity through the shelterbelt and d_e is the average diameter of vegetation elements within the shelterbelt. Figure 8 shows the efficiency of three vegetation element sizes spanning the range encountered in a shelterbelt as a function of the incoming droplet diameter. As has previously been noted [9] small vegetation elements have a better capture efficiency since the flow around them is deflected less than that for large elements so the droplets have a higher probability of hitting the element and being captured. Also since the larger droplets have greater inertia they also have higher capture efficiency.

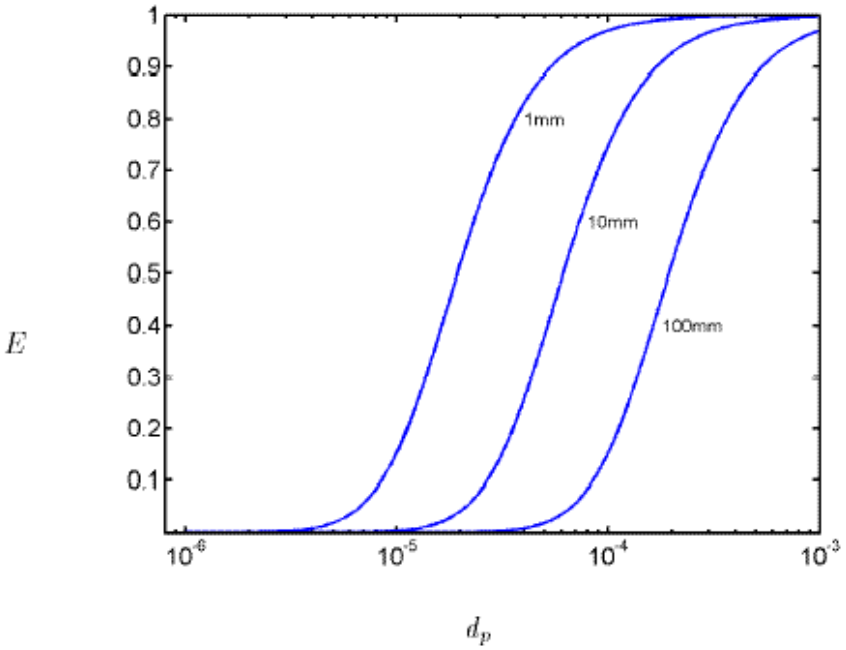

Figure 8. Capture efficiency versus droplet diameter for three vegetation element sizes covering the range encountered (d_e = 1, 10 and 100mm) with a bleed velocity of U_b = 1 m/s.

4.2. Total capture efficiency

Now that we have a means of determining the capture efficiency of an individual vegetation element we wish to determine the capture efficiency across the shelterbelt. Let C be the particle concentration in the shelterbelt with C_0 the upwind edge concentration and C_W the downwind edge concentration. The quantity of interest is the total capture efficiency of the shelterbelt, namely

$$T = \frac{C_0 - C_W}{C_0} \tag{11}$$

when expressed as a ratio of the incoming concentration. The concentration through the shelterbelt (neglecting diffusion through it) is governed

by the differential equation

$$\frac{dC}{dt} = -AEU_b C\,, \tag{12}$$

where A is the frontal area of the vegetation elements per unit volume and EU_b is the impaction conductance onto vegetation elements. Integrating across the shelterbelt gives

$$T = 1 - \frac{C_W}{C_0} = 1 - \exp(-AEU_b\bar{t})\,, \tag{13}$$

where $\bar{t}$ is a typical time to cross the shelterbelt. Since the flow within the shelterbelt is turbulent, $\bar{t}$ is not simply W/U_b but longer as the flow meanders through the shelterbelt. Define

$$\bar{t} = M\frac{W}{U_b}\,, \tag{14}$$

where M is a meander factor based on the turbulence. [6] take $M = 1.2$.The constant A is not easily measured in the field for a given shelterbelt. A more natural measurement used is the *optical* porosity (τ) of the shelterbelt which is related to A by

$$\tau = \exp(-AW). \tag{15}$$

Substituting (14) and (15) into (13) then gives the total capture efficiency of the shelterbelt as a function of the optical porosity and the physical parameters used in determining E as

$$T = 1 - \tau^{EM}. \tag{16}$$

Figure 9 shows the total capture efficiency as given by equation (16) for two different types of shelterbelt (dashed lines are a needle like shelterbelt with element size of 1 mm, solid lines are an intermediate shelterbelt with element size of 10 mm) for a *given* bleed velocity of 1 m/s. For each type of curve the four curves are for droplet sizes of 20, 40, 80 and 160 μm, increasing vertically on the plot. The small vegetation element shelterbelt clearly outperforms the larger element shelterbelt particularly for the smaller droplet sizes.

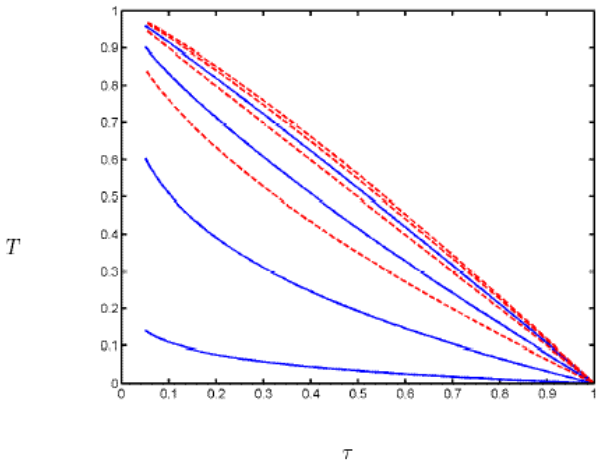

Figure 9. Total capture efficiency versus optical porosity for two vegetation element sizes (solid lines 10 mm, dashed lines 1mm) covering the range of droplet sizes encountered (20, 40, 80 and 160 m, increasing vertically on the plot) with a given bleed velocity of $U_b = 1$ m/s.

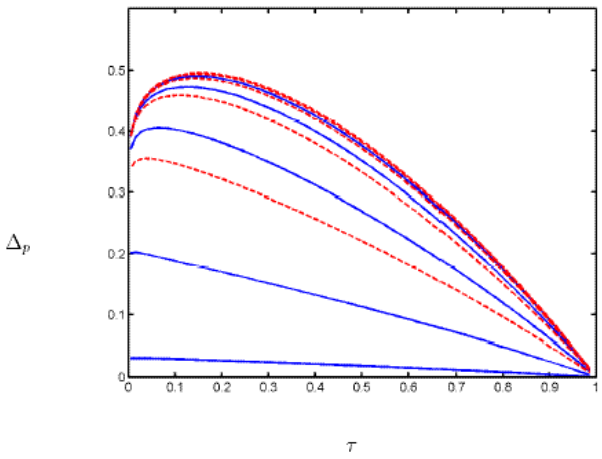

Figure 10. Nondimensional deposition rate efficiency versus optical porosity for two vegetation element sizes (solid lines 10 mm, dashed lines 1mm) covering the range of droplet sizes encountered (10, 20, 40, 80 and 160 m, increasing vertically on the plot) with a mean ambient velocity of $U = 5$ m/s.

Figure 9 should be viewed with caution since it is plotted for a *given* bleed velocity. The bleed velocity is actually a function of the porosity of the shelterbelt which should be taken into account. If the bleed velocity is known, for example from measurements just downstream of the shelterbelt or from Section 2, then the analysis to date is sufficient for operational use. In practice the bleed velocity is difficult to measure accurately and so an approximation to it based on the characteristics of the shelterbelt and the ambient wind needs to be determined.

4.3. Bleed velocity

The determination of the bleed velocity through the shelterbelt is important in being able to model the efficiency of collection spray drift of a shelterbelt. Of most practical interest is the ability to be able to determine the bleed velocity (and hence the efficiency of the shelterbelt) from easily measured or estimated variables. For a particular operational case a measurement (if possible) of the bleed velocity is appropriate. As an example, a farmer may wish to determine the efficiency of a particular shelterbelt in a particular wind in which case a direct measurement of the bleed velocity can be used in the preceeding formulas to determine the shelterbelt efficiency. Note that this still requires an estimate of the optical porosity of the shelterbelt and other physical parameters such as the range of droplet sizes, shelterbelt element size and the like. Direct measurement of the bleed velocity raises questions such as: where should these measurements be taken? are the instruments accurate enough at such low velocities? how many measurements need to be taken to obtain a consistent value? etc. In general, of more practical use is to determine an estimate of the bleed velocity in terms of the ambient wind and optical porosity. This approach has two main advantages. In an operational setting the less data that has to be collected the more likely the procedure is to be used and less measurement induced error is therefore included. In a planning setting different scenarios (shelterbelt structure, wind profile, droplet distribution, etc.) can be tested with a view to determining some overall guidelines.

[6] gives a detailed description of the calculation of the determination of the bleed velocity which will be summarised here. If the unobstructed mean wind speed is U then by considering the drag on the shelterbelt and on individual shelterbelt elements [6] derives the bleed velocity

$$U_b = U\left(\frac{\Gamma}{\Gamma k_1 + k}\right)^{1/2}, \tag{17}$$

where the parameters Γ and k_1 are determined from semi-empirical grounds based on the two extremes of dense and sparse shelterbelts.

Γ is found to be in the range 1.0 to 1.1 with a typical value that agrees with experiments of 1.07. The dependence on k_1 is quite weak and a value of 1.5 is found to be satisfactory. The variable k is a measure of the drag of individual vegetation elements and is

$$k = -C_e \log \tau \,, \tag{18}$$

where C_e is the drag coefficient of individual elements which over the range of sizes, shapes and wind speeds considered here is well approximated by 1 [3].

4.4. Deposition rate

Combining equation (17) and the capture efficiency equation (13) we get a measure of the depostion rate per unit width of the shelterbelt (kg(ms)$^{-1}$) onto a shelterbelt of height L:

$$\begin{aligned} D_p &= LC_0U_bT \\ &= LC_0U\left(\frac{\Gamma}{\Gamma k_1 - \log\tau}\right)^{1/2}\left(1-\tau^{EM}\right) . \end{aligned} \tag{19}$$

For a given practical situation where all the physical factors such as shelterbelt dimensions and structure (vegetation element size, optical porosity), wind speed, spray drift concentration and droplet distribution are known equation (19) can be used to determine the deposition rate onto the shelterbelt elements. For comparative and planning purposes it is better to nondimensionalise equation (19) relative to a completely transparent shelterbelt (that is as if the shelterbelt was not collecting any spray drift and not interrupting the flow) and some reference concentration C_0. This reduces the number of variables and gives a measure of the overall efficiency of a shelterbelt compared to no shelterbelt at all. The nondimensional measure is

$$\Delta_p = \left(\frac{\Gamma}{\Gamma k_1 - \log\tau}\right)^{1/2}\left(1-\tau^{EM}\right). \tag{20}$$

This depends in the obvious way on the optical porosity (τ) and through E on the ambient mean wind, the structure of the shelterbelt, and the distribution of the spray drift droplet sizes. There is clearly a trade off in the efficiency of the shelterbelt given by equation (20) in terms of the optical porosity. A dense shelterbelt (low τ) has a low bleed velocity (the first term) but a high capture efficiency (the second term) whereas a sparse shelterbelt (high τ) has a high bleed velocity but a low capture efficiency. This is shown in Figure 10 which is a

plot of Δ_b for $U = 5\,\mathrm{m/s}$ for 2 different vegetation element sizes (solid lines 10 mm, dashed lines 1 mm) and 5 different droplet sizes (10, 20, 40, 80 and 160 μm). In this example there is a range of optical porosity around $\tau = 0.15$ where the competing effects give a maximum deposition. Again it is clear that the small droplets are not captured particularly well by the larger vegetation elements.

4.5. Ambient wind effects

The effect of different ambient winds on the capture efficiency of the shelterbelt needs to be determined. Farmers typically do not spray in very light winds (< 1 m/s) as the spray drift direction is too uncertain or in very high winds (> 5 m/s) as the downwind spray drift is considered to be too large. As mentioned in Section 2.2 the geometry of the air flow is largely independent of the ambient wind velocity U. So for a shelterbelt of given porosity the same percentage of the flow goes through the shelterbelt independent of the wind velocity. What is effected is the bleed velocity U_b as it is directly proportional to U (equation (17)) and hence the capture efficiency of the shelterbelt. Ignoring factors such as streamlining of vegetation elements higher bleed velocities capture a higher percentage of the spray drift since the spray drift droplets have less time to deviate in the flow and hence impact on the vegetation. Hence higher wind velocities should see a higher capture efficiency of the shelterbelt.

Tables 2 and 3 is an example of the type of information that will be supplied to users of this model. It gives the efficiency for 7 different shelterbelt types at 5 different ambient wind velocities. The shelterbelts range from large element poplar (both full canopy and pruned versions), medium element but very dense Cryptomeria, small element Casuarina, Willow in both summer (leaves on) and winter (leaves off) form and an artifical netting shelterbelt. Note that for the artificial shelterbelt the meander factor M was set to unity since it is very thin and hence does not force the flow to meander as the other shelterbelts do. The increase in capture efficiency with the increasing wind velocity is evident as is the low efficiency of capture of the smaller droplets.

4.5.1 Streamlining. Streamlining of vegetation elements has the opposite effect as higher winds lead to more streamlining which increases the optical porosity of the shelterbelt making it less efficient at spray drift collection. Streamlining is more pronounced for smaller vegetation elements. [6] derived a formula for the change in the porosity due to the streamlining by balancing the turning moment of a vegetation

Table 2. Capture efficiency for 7 different typical shelterbelt types for a range of droplet sizes at 5 wind velocities

Shelterbelt Type and Structure	Droplet size (μm)	$U_H = 1\,\mathrm{m/s}$	$U_H = 2\,\mathrm{m/s}$	$U_H = 3\,\mathrm{m/s}$	$U_H = 4\,\mathrm{m/s}$	$U_H = 5\,\mathrm{m/s}$
Poplar d_e = 100mm Porosity $\tau = 0.2$ Moderately Dense	$10-30$	< 0.01	< 0.01	< 0.01	< 0.01	< 0.01
	40	< 0.01	0.01	0.02	0.04	0.06
	50	< 0.01	0.03	0.05	0.08	0.10
	75	0.03	0.09	0.14	0.19	0.23
	100	0.08	0.17	0.24	0.29	0.32
	125	0.13	0.25	0.31	0.35	0.38
	150	0.19	0.31	0.36	0.39	0.41
	200	0.29	0.38	0.42	0.44	0.45
Pruned Poplar d_e = 100mm Porosity $\tau = 0.5$ Sparse	$10-30$	< 0.01	< 0.01	< 0.01	< 0.01	< 0.01
	40	< 0.01	< 0.01	0.02	0.03	0.04
	50	< 0.01	0.02	0.03	0.05	0.07
	75	0.02	0.06	0.10	0.13	0.15
	100	0.05	0.11	0.16	0.20	0.22
	125	0.09	0.17	0.21	0.25	0.27
	150	0.13	0.21	0.25	0.28	0.30
	200	0.20	0.27	0.30	0.32	0.33
Cryptomeria d_e = 1 − 5mm Porosity $\tau = 0.02$ Very Dense	10	$0.01-0.09$	$0.02-0.20$	$0.04-0.28$	$0.07-0.32$	$0.09-0.35$
	20	$0.06-0.32$	$0.16-0.39$	$0.24-0.41$	$0.29-0.42$	$0.32-0.43$
	30	$0.18-0.40$	$0.31-0.42$	$0.36-0.43$	$0.39-0.43$	$0.40-0.43$
	40	$0.29-0.42$	$0.38-0.43$	$0.40-0.43$	0.43	0.43
	50	$0.35-0.43$	$0.41-0.43$	0.43	0.43	0.44
	75	$0.41-0.43$	0.43	0.44	0.44	0.44
	100 − 200	0.43	0.43	0.44	0.44	0.44
Casurina d_e = 2mm Porosity $\tau = 0.2$ Moderately Dense	10	0.03	0.08	0.13	0.17	0.21
	20	0.17	0.28	0.35	0.38	0.40
	30	0.31	0.39	0.43	0.44	0.45
	40	0.38	0.44	0.46	0.47	0.47
	50	0.42	0.46	0.47	0.48	0.48
	75	0.46	0.48	0.48	0.49	0.49
	100 − 200	0.48	0.49	0.49	0.49	0.49

Table 3. Capture efficiency for 7 different typical shelterbelt types for a range of droplet sizes at 5 wind velocities

Shelterbelt Type and Structure	Droplet size (μm)	$U_H = 1\,\mathrm{m/s}$	$U_H = 2\,\mathrm{m/s}$	$U_H = 3\,\mathrm{m/s}$	$U_H = 4\,\mathrm{m/s}$	$U_H = 5\,\mathrm{m/s}$
Matsudana Willow	10	< 0.01	< 0.01	$0 - 0.02$	$0 - 0.03$	$0 - 0.04$
$d_e = 3 - 40$mm	20	$0 - 0.03$	$0 - 0.06$	$0 - 0.08$	$0.01 - 0.10$	$0.03 - 0.14$
Porosity $\tau = 0.8$	30	$0 - 0.07$	$0 - 0.11$	$0.01 - 0.12$	$0.03 - 0.14$	$0.05 - 0.16$
Winter(leaves off)	40	$0.01 - 0.10$	$0.02 - 0.13$	$0.03 - 0.14$	$0.04 - 0.15$	$0.07 - 0.17$
Very Sparse	50	$0.02 - 0.12$	$0.03 - 0.15$	$0.05 - 0.15$	$0.06 - 0.16$	$0.11 - 0.17$
	75	$0.03 - 0.15$	$0.07 - 0.16$	$0.09 - 0.16$	$0.10 - 0.17$	$0.14 - 0.18$
	100	$0.06 - 0.16$	$0.10 - 0.17$	$0.12 - 0.17$	$0.13 - 0.17$	$0.15 - 0.18$
	125	$0.08 - 0.17$	$0.12 - 0.17$	$0.14 - 0.17$	$0.14 - 0.18$	$0.15 - 0.18$
	150	$0.10 - 0.17$	$0.13 - 0.18$	$0.15 - 0.18$	$0.15 - 0.18$	$0.16 - 0.18$
	200	$0.13 - 0.17$	$0.15 - 0.18$	$0.16 - 0.18$	$0.16 - 0.18$	$0.17 - 0.18$
Artificial	10	0.02	0.04	0.07	0.10	0.12
$d_e = 1 - 2$mm	20	0.10	0.17	0.21	0.23	0.25
Porosity $\tau = 0.5$	30	0.18	0.24	0.27	0.29	0.30
Meander Factor=1	40	0.23	0.28	0.30	0.31	0.32
	50	0.31	0.30	0.31	0.32	0.33
	75	0.32	0.32	0.33	0.33	0.34
	100 – 200	0.33	0.33	0.34	0.34	0.34
Matsudana Willow	10	< 0.01	< 0.01	< 0.01	< 0.01	< 0.01
$d_e = 15 - 50$mm	20	< 0.01	$0 - 0.03$	$0.01 - 0.06$	$0.01 - 0.08$	$0.02 - 0.11$
Porosity $\tau = 0.2$	30	$0.01 - 0.04$	$0.02 - 0.10$	$0.03 - 0.15$	$0.05 - 0.20$	$0.07 - 0.24$
Summer(leaves on)	40	$0.01 - 0.08$	$0.04 - 0.18$	$0.07 - 0.25$	$0.10 - 0.30$	$0.14 - 0.33$
Moderately Dense	50	$0.03 - 0.14$	$0.08 - 0.26$	$0.12 - 0.32$	$0.17 - 0.36$	$0.21 - 0.39$
	75	$0.09 - 0.27$	$0.19 - 0.37$	$0.26 - 0.41$	$0.31 - 0.43$	$0.34 - 0.45$
	100	$0.17 - 0.36$	$0.29 - 0.43$	$0.35 - 0.45$	$0.38 - 0.46$	$0.40 - 0.47$
	125	$0.25 - 0.41$	$0.35 - 0.43$	$0.40 - 0.46$	$0.42 - 0.47$	$0.44 - 0.48$
	150	$0.31 - 0.43$	$0.39 - 0.46$	$0.43 - 0.47$	$0.44 - 0.48$	$0.45 - 0.48$
	200	$0.38 - 0.46$	$0.44 - 0.48$	$0.46 - 0.48$	$0.47 - 0.49$	$0.47 - 0.49$

element with its drag assuming the vegetation element is a suspended stick free to turn (this is a worst case scenario and in general vegetation is more resistant to streamlining than this) Their equation is

$$\tau(U_b) = \tau_0^{\cos\theta}\,, \tag{21}$$

where τ_0 is the unstreamlined value for the optical porosity and

$$\cos\theta = \left(1 + \left(\frac{2\rho_a C_e U_b^2}{\pi \rho_e g d_e}\right)^2\right)^{-1/2} \tag{22}$$

where ρ_e is the density of the vegetation element. Over the range of wind velocities relevant here the streamlining is only relevant for vegetation elements smaller than about 5 mm. This is shown by Figure 11 where values of $\cos\theta$ significantly different from 1 result in streamlining being important. It should be remembered that U_b is considerably less than U when interpreting this diagram in terms of the ambient wind.

Combining all of the above effects it is possible to determine a range of optical porosities and wind speeds to maximize the capture efficiency of a shelterbelt for a given droplet distribution. As an example taking a typical droplet distribution from a sprayer (Forster, private communication), allowing for 10 seconds of evaporation at RH = 80 and settling time with a cutoff size of 150 μm and then applying the above gives Figure 12. Three ambient wind velocities are considered (solid lines $U = 1$ m/s, dashed lines $U = 3$ m/s, dot-dash lines $U = 5$ m/s) and three diferent vegatation element sizes (diamonds 100 mm, triangles 10 mm, squares 1 mm) and streamlining is also considered for the 1 mm vegetation elements (circles). The effect of the ambient wind strength is obvious. Ignoring streamlining the stronger the ambient wind the better the capture efficiency particularly for the larger vegetation elements. For the smallest vegetation element the wind velocity has a negligible effect unless streamlining is a factor. When streamlining is allowed for the performance of the 1 mm vegetation element shelterbelt deteriorates considerably for the high wind velocities. Generally the shelterbelt performs best over a range of optical porosities from 0.1 to 0.3 and for small vegetation elements particularly if they are made up of elements that do not streamline easily.

4.5.2 Wind at an angle. An underlying assumption in the above modelling is that the wind is perpendicular to the shelterbelt and that the flow through the shelterbelt is also on average perpendicular with some meandering allowed due to the turbulent flow. If the incoming wind is at an angle to the shelterbelt then this needs to be

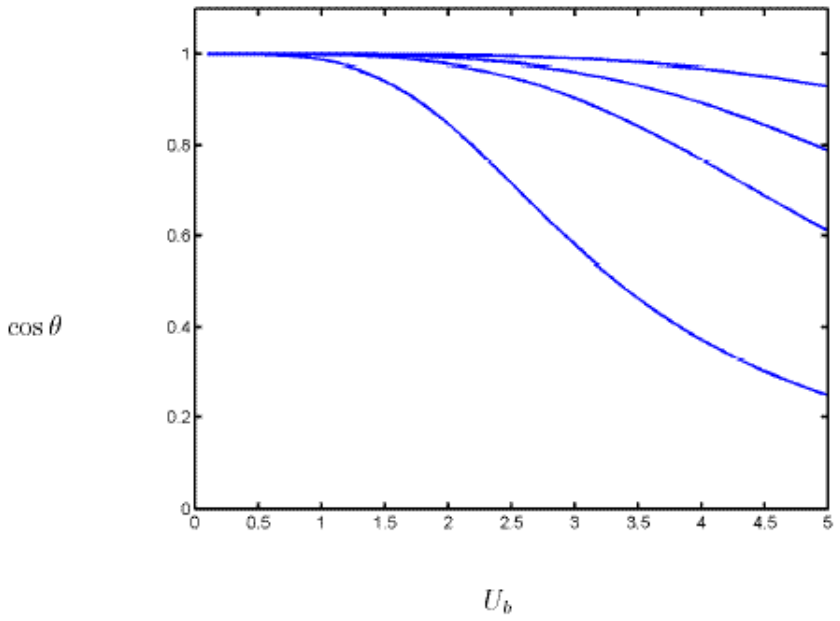

Figure 11. Changes in the porosity due to streamlining given by the power coefficient of the optical porosity versus the bleed velocity for vegetation elements of size 1, 3 5 and 10 mm, increasing vertically on the plot. Values significantly different from 1 show that streamlining is an important factor.

compensated for. [11] gives a good review of the literature available on this topic. A typical wind profile through the shelterbelt is given in Figure 13. Ahead of the shelterbelt the air rotates toward the direction parallel to the shelterbelt then makes an abrupt turn and passes almost perpendicular through the shelterbelt before exiting the shelterbelt and rotating back to the incident angle. The degree of rotation is governed by the wind speed, the porosity and the height up the shelterbelt. The reason the wind passes through the shelterbelt almost perpendicular is that the pressure gradient across the shelterbelt is perpendicular to the shelterbelt and hence the flow tries to follow the pressure gradient. The fact that the flow through the shelterbelt is perpendicular means that the above modelling is still valid for incident winds at an angle provided the velocity is suitably reduced. Although the precise reduction in velocity is a complicated and little understood function of factors such as the

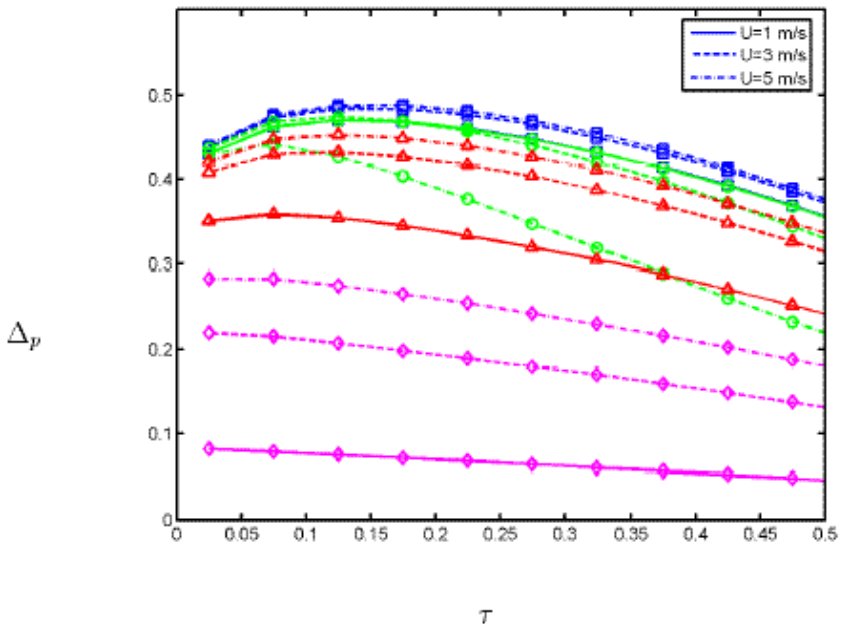

Figure 12. Nondimensional deposition rate efficiency versus optical porosity for three ambient wind velocities (solid lines U = 1 m/s, dashed lines U = 3m/s, dot-dash lines U = 5m/s) and three vegetation element sizes (diamonds 100 mm, triangles 10 mm, squares 1mm) and streamling in the 1mm case (circles).

porosity and angle (see [11]) it is sufficient for the scope of this project to just take the perpendicular component of the wind as the velocity U used previously, hence

$$U = U_i \cos(\phi)\,, \tag{23}$$

where ϕ is the angle of incidence (see Figure 13) and U_i is the incident wind speed.

5. Conclusion

In conclusion the MISG team have verified that an existing model as developed by [6] was suitable for use in determining the efficiency of a shelterbelt at collecting spray drift. The model is relatively simple to program and uses as inputs easily obtainable variables such as the free stream wind velocity, the optical porosity of the shetlerbelt and the structure of the shelterbelt. With allowances for settling and

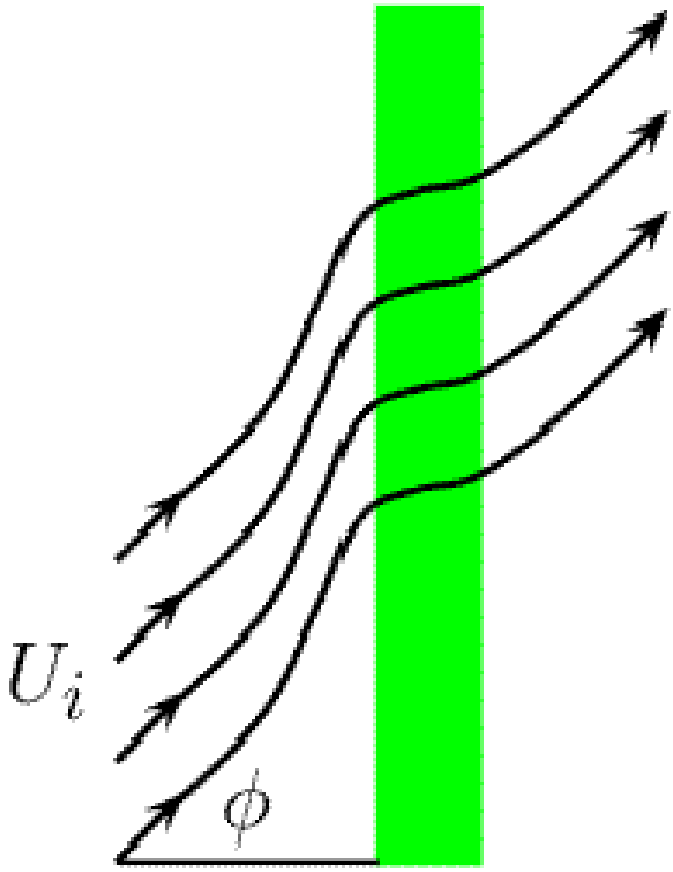

Figure 13. Typical streamlines when the wind is at an angle ϕ to the shelterbelt as viewed from above.

evaporation the model was found to be valid over the range of inputs typically found for droplet distribution, wind velocity and vegetation element size. Numerical simulations of the flow field over and through the shelterbelt have justified some of the assumption used in the model and given insight into the flow characteristics that are important to consider. Although these models are never perfect representations of the real world we believe they are suitably robust for inclusion in a larger

spray drift management system. Although care must be taken to ensure that some of the original assumptions are not overly breached.

Further work on determining the optimal shelterbelt is also possible. This has implications to the design of artificial shelterbelts where the highest possible spray drift capture is desired.

Notes

1. The quadratic drag law is appropriate for most realistic flow speeds [3] as the Reynolds number Re $\sim 5,000$ for a leaf diameter of 5 cm and flow speed of say 1 m/s. The factor ℓ is some length scale of the drag law discussed soon.

2. The zero in eddy diffusivity as $y \to 0$ is sequestered harmlessly away at the bottom of the crop.

References

[1] Biferale, L. (2003), *Shell models of energy cascade in turbulence*, Annu. Rev. Fluid Mechanics 35, 441-468.

[2] Britter, R. E. and Hanna, S. R. (2003), *Flow and dispersion in urban areas*, Annu. Rev. Fluid Mechanics 35, 469-496.

[3] Hughes, W. F. and Brighton, J. A. (1999), Schaums outlines: theory and problems of fluid dynamics, 3 edn, McGrawHill.

[4] Landahl, M. T. and Mollo-Christensen, E. (1986), Turbulence and random processes in fluid mechanics, Cambridge University Press.

[5] Peters, K. and Eiden, R. (1992), *Modelling the dry deposition velocity of aerosol particles to a spruce forest*, Atmospheric Environment 26A, 2555-2564.

[6] Raupach, M. R., Woods, N., Dorr, G., Leys, J. F. and Cleugh, H. A. (2001), *The entrapment of particles by windbreaks*, Atmospheric Environment 35, 3373-3383.

[7] Richardson, L. F. (1926), *Atmospheric diffusion shown on a distance-neighbour graph*, Proc. R. Soc.London Ser. A. 110, 709–737.

[8] Speziale, C. G. (1991), *Analytical methods for the development of reynoldsstress closures in turbulence*, Annu. Rev. Fluid Mech. 23, 107-157.

[9] Ucar, T., Hall, F. R., Tew, J. E. and Hacker, J. K. (2003), *Wind tunnel studies on spray deposition on leaves of tree species used for windbreaks and exposure of honey bees*, Pest Management Sci. 59, 358-364.

[10] Wake, G. (2004), The relative humidity effect on aerosoal drolet transport and consequential pollutant dispersal, Technical report, Massey University.

[11] Wang, H., Tackle, E. S. and Shen, J. (2001), *Shelterbelts and windbreaks: mathematical modeling and computer simulations of turbulent flows*, Annu. Rev. Fluid Mech. 33, 549-586.